Journal of Catalysis 285 (2012) iii–xi

Contents lists available at SciVerse ScienceDirect

Journal of Catalysis

journal homepage: www.elsevier.com/locate/jcat

Journal of Catalysis Vol. 285, Issue 1, 2012

Contents

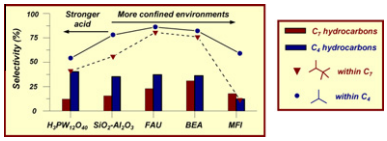

Formation of isobutane and triptane from C_1 precursors is favored on all solid acids, because methylation and hydride transfer steps selectively grow hydrocarbons without significant deviations via isomerization steps. Triptane and isobutane selectivities are maximized on BEA and FAU because weak acid sites and confinement within large channels preferentially stabilize hydride transfer and methylation transition states that preserve the structure of triptane in growing hydrocarbons over isomerization transition states.

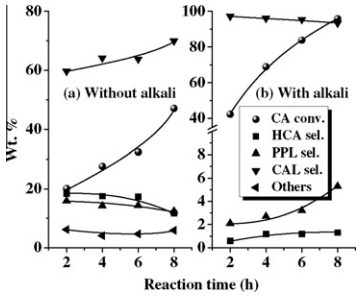

Selective liquid phase hydrogenation of cinnamaldehyde is reported, for the first time, over CeO_2–ZrO_2-supported Pt catalysts, which are highly active and selective even at 25 °C.

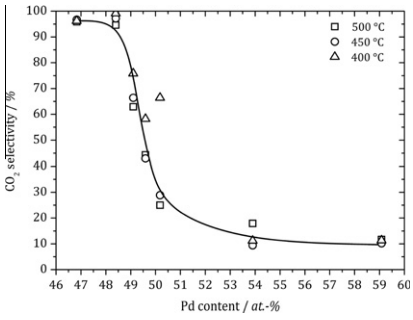

Methanol steam reforming was studied on unsupported ZnPd intermetallic compounds with different compositions proving Zn-rich compounds to show excellent CO_2 selectivity compared to Pd-rich compounds.

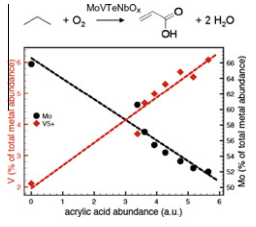

The surface of a highly crystalline MoVTeNb oxide catalyst composed exclusively of the M1 phase has been studied before catalysis and during operation in oxidation of propane at 693 K. Increasing formation of acrylic acid in general goes along with surface depletion of Mo and accordingly the enrichment in Te, V, and Nb. A close correlation exists between the acrylic acid production and the increasing presence of surface V^{5+} species.

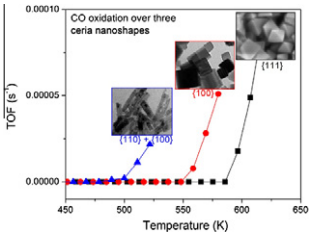

Not only the interaction between CO and ceria but also the reactivity and mobility of lattice oxygen in ceria are greatly influenced by the surface structure of ceria, leading to the strong variation in CO oxidation over ceria nanoshapes.

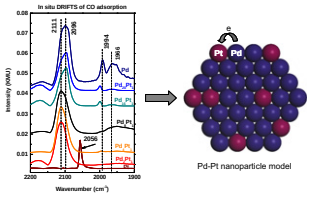

H_2O_2 synthesis directly from H_2 and O_2 over supported Pd–Pt alloy catalysts was studied using a tri-phase reactor under ambient conditions. $Pd_{16}Pt_1$ showed the best performance with a rate of 1.77 mol h^{-1} g_{Pd}^{-1} and a selectivity of 60% while 0.99 mol h^{-1} g_{Pd}^{-1} and only 12% observed for pure Pd.

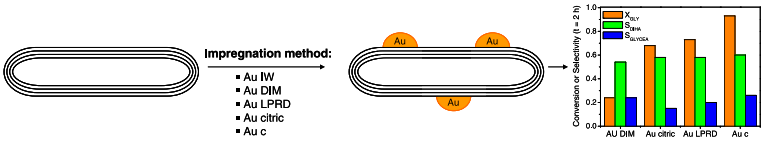

A remarkable high selectivity to dihydroxyacetone combined with a high activity is obtained in the glycerol oxidation over Au/MWCNT catalysts, particularly if the sol immobilization technique is used for the impregnation of gold.

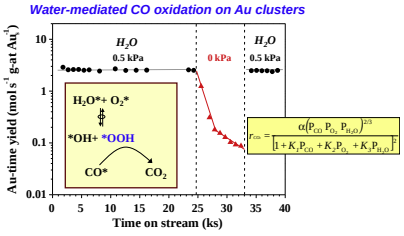

Kinetic and isotopic data show that H_2O acts as a co-catalyst for the activation of O_2 and the retention of catalytic reactivity in CO oxidation on Au clusters. H_2O mediates O_2 activation steps, circumvents the kinetic bottlenecks prevalent under anhydrous conditions, and accounts for the remarkable reactivity of monofunctional Au metal clusters at near ambient temperatures.

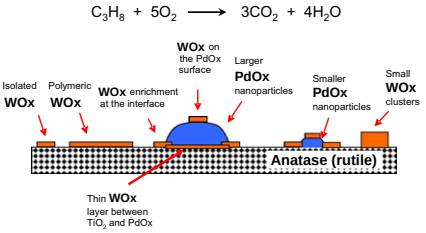

Titania-supported palladium catalysts modified by the addition of tungsten were studied for the total oxidation of propane. The addition of tungsten significantly improved catalyst performance, and this is related to the structure of the catalyst.

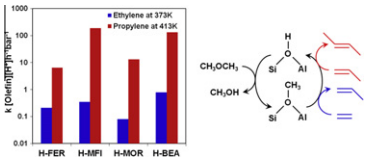

Dimethyl ether methylation of olefins proceeds via the same mechanistic pathway on different zeolites, but with different rates of reaction showing that zeolites propagate olefin methylation reaction cycles prevalent in methanol-to-hydrocarbons conversion to varying extents. The formation and involvement of surface methoxide species is consistent with the secondary kinetic isotope effect observed using CD_3OCD_3 reactants and with olefin methylation rates having a zero-order dependence in DME pressures and a first-order dependence in olefin pressure.

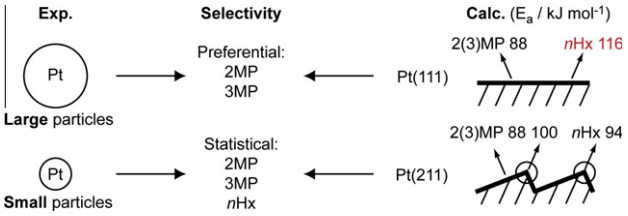

Methylcyclopentane is a benchmark model system to study selective ring-opening of hydrocarbons on supported Pt. Electronic structure calculations show that the distribution of possible ring-opening products, *n*-hexane (*n*Hx) and its branched isomers, 2- and 3-methylpentane (2MP and 3MP), is controlled by the height of the C–C bond scission barrier.

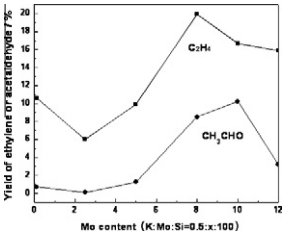

Potassium-modified K/Mo-SBA-15 catalysts give supercatalytic performance for the selective oxidation of ethane to acetaldehyde and ethylene. The maximum yields of acetaldehyde and ethylene can reach 10.2% and 19.9%, respectively.

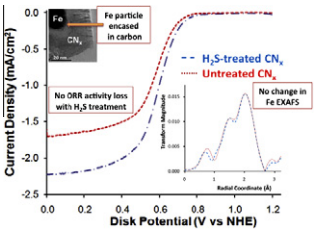

Examining the role of Fe in CN_x materials for oxygen reduction reaction by deliberate poisoning with H_2S.

The O_2 plasma working under mild conditions can remove the organic compounds efficiently without causing aggregation of gold nanoparticles. The O_2 plasma-treated Au/SiO_2 showed good catalytic performances in the selective hydrogenation of C_2H_2 in large excess of C_2H_4 at low temperature, which might be due to the small size and the nearly neutral charge of gold nanoparticles.

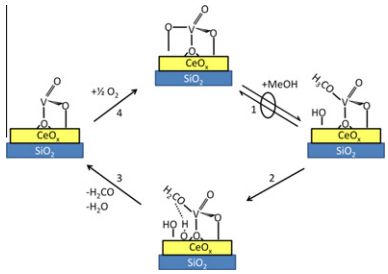

An investigation of methanol oxidation to formaldehyde was carried out using bilayered $VO_x/CeO_2/SiO_2$ catalysts consisting of pseudo-tetrahedral vanadate species supported on an amorphous ceria layer. The activity of $VO_x/CeO_2/SiO_2$ was about 20-fold higher than that of VO_x/SiO_2. This difference is attributed to the differences in the rate-limiting step for formaldehyde formation on the two catalysts.

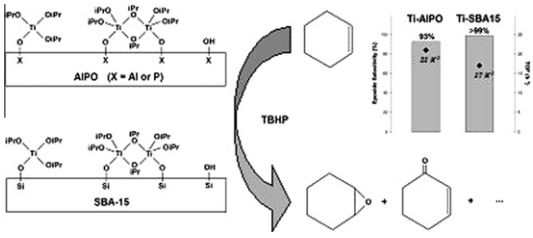

Mesoporous aluminophosphates were grafted by titanium isopropoxide and investigated as catalysts for the oxidation of cyclohexene. The Ti-AlPO catalysts have comparable structural and catalytic properties than similar Ti-SBA15 catalysts, but exhibit a higher tendency toward allylic oxidation.

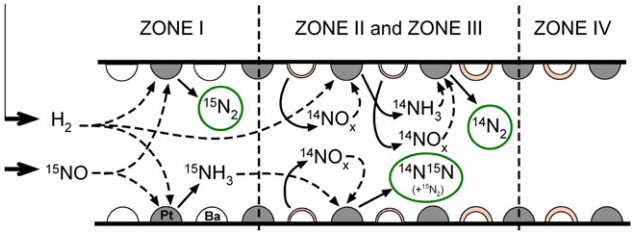

The evolution of products formed from reduction of stored nitrates on a Pt–Ba/Al_2O_3 LNT catalyst is significantly modified by the presence of NO during the regeneration. Isotope labelling techniques allowed us to propose three different routes for N_2/NH_3 formation; extension of which is affected by the H_2 concentration.

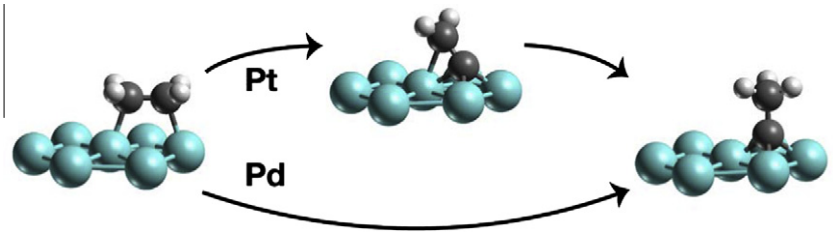

kMC Simulations predict that the most plausible pathway on the Pd(1 1 1) and Pt(1 1 1) surfaces is ethylene → vinyl → vinylidene → ethylidyne.

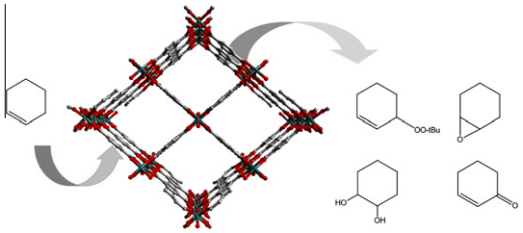

V-MIL-47 is evaluated as a catalyst in the epoxidation of cyclohexene. Experimental results, combined with computational modelling confirm that at least two parallel catalytic cycles are co-existing: one with V+IV sites and one with pre-oxidized V+V sites.

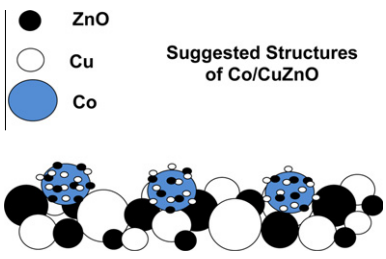

ZnO and Cu decorate the Co surface, blocking a substantial number of active sites on Co for CO hydrogenation.

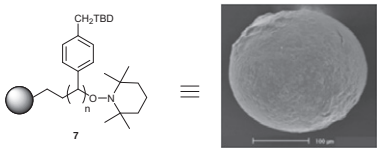

In this contribution Rasta polymer has been used to preparation of high-loading Rasta-TBD. This catalyst has been able to efficiently promote several organic transformations with constantly good and promising results.

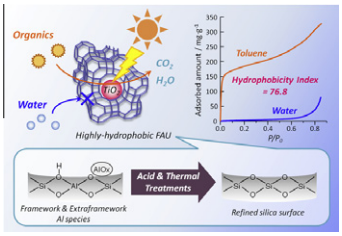

Faujasite zeolite of high crystallinity, stability, and hydrophobicity improves the photocatalytic degradation of 2-propanol in water and acetaldehyde in air when used as catalyst support for TiO_2.

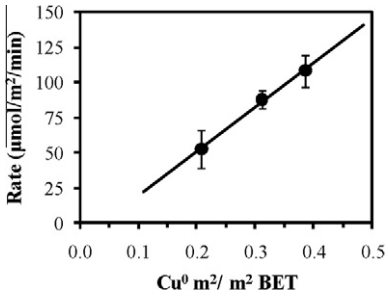

The roles of the Cu^0 and Cu^+ species in a copper chromite catalyst, $CuCr_2O_4$·CuO, in the condensed-phase hydrogenolysis of 5-methylfurfuryl alcohol to 2,5-dimethylfuran were investigated. The maxima of both active species occurred after reduction at 300 °C for 1 h. The correlation between Cu^0 and specific activity suggested that Cu^0 was primarily responsible for catalytic activity.

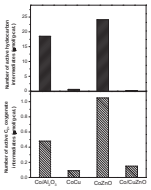

Compared to Co/Al_2O_3, the addition of Cu to Co decreases the concentrations of active surface intermediates significantly for both hydrocarbons and C_{2+} oxygenates while those quantities can increase somewhat with ZnO. The high selectivities for C_{2+} oxygenates observed for Co/CuZnO are due to the low concentration of active surface intermediates for hydrocarbons relative to that for oxygenates.

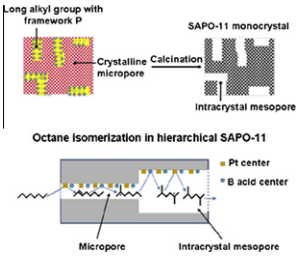

The P atoms in alkylphosphonic acid are introduced into the SAPO-11 framework, and thus the long alkyl groups bonded with these P atoms induce the formation of intracrystal mesopores after calcination. The interpenetrating micro–mesoporous channels of the hierarchical SAPO-11 endow the resulting catalyst with the superior di-branched isomer selectivity.

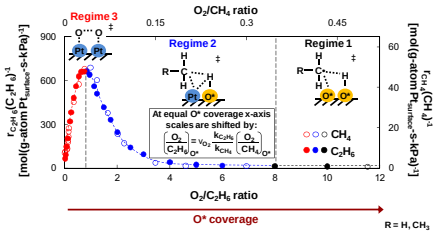

Kinetic and isotopic data and Pt cluster size effects show that C_2H_6—O_2 and CH_4—O_2 form CO_2 and H_2O via analogous elementary steps; turnover rates are higher for C_2H_6 in all kinetic regimes where C—H bond cleavage limits rates because weaker C—H bonds in C_2H_6 and stronger ethyl interactions with adsorbed oxygens (O^*) at transition states lead to lower barriers for C_2H_6 than for CH_4 activation. Reactivity differences cause transitions between kinetic regimes to occur at higher O_2/alkane ratios for C_2H_6 because it scavenges O^* species more effectively than CH_4 and leads to lower O^* coverages. These mechanistic analogies and insights can be rigorously extended to other alkanes and metal clusters.

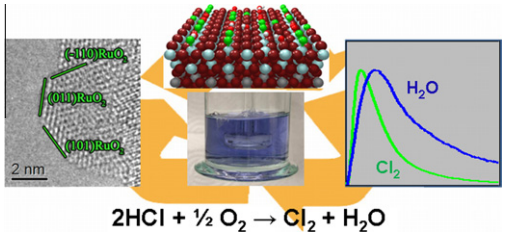

By using state-of-the-art experiments and theoretical calculations, we unravel mechanistic details of HCl oxidation on the industrially relevant RuO_2/SnO_2 catalyst. On the extensively chlorinated surface, oxygen activation is the rate determining step.

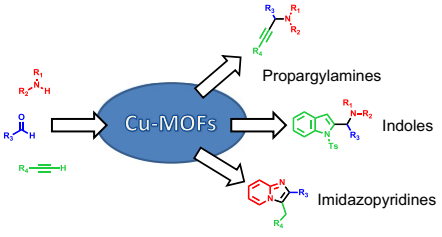

Copper-containing MOFs are highly active catalysts for one-pot three-component coupling reactions of amines, alkynes and aldehydes to form propargylamines. When an additional intramolecular cyclization step is included, indole and imidazopyridines can also be efficiently formed.

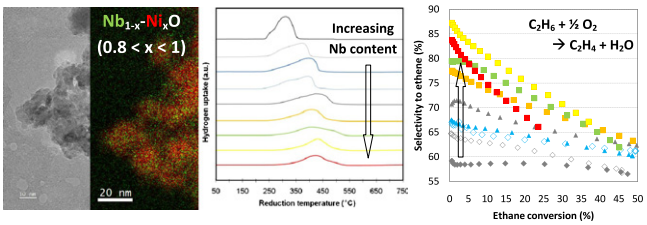

Nb-NiO nanocomposites, which are prepared with a high surface area for the first time, prove highly active for low temperature ethane ODH. Structural and catalytic properties are discussed as a function of the Nb content.

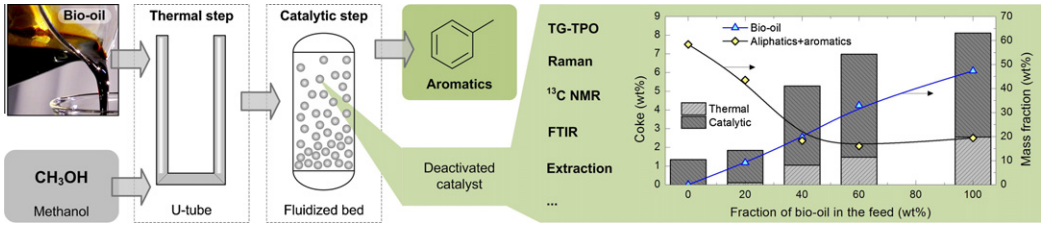

The nature of the coke deposited on a HZSM-5 catalyst (modified with Ni) in the transformation of crude bio-oil was studied. Co-feeding methanol attenuates coke deposition and affects the heterogeneous and oxygenated nature of the coke.

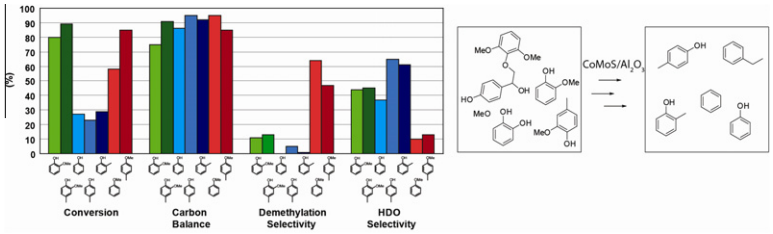

Extensive hydrodeoxygenation studies with a sulfided $CoMo/Al_2O_3$ catalyst were performed on a library of lignin model compounds. An extended reaction network is proposed, showing that HDO, demethylation, and hydrogenation reactions take place simultaneously.

NOTE

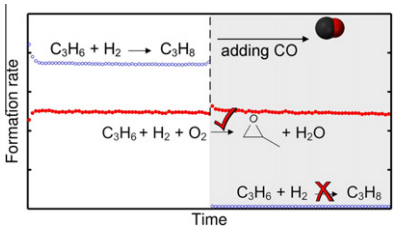

Carbon monoxide switches off propene hydrogenation in the direct epoxidation of propene with hydrogen and oxygen over $Au/Ti–SiO_2$ catalysts.